Journal of Materials Chemistry A

Accepted Manuscript

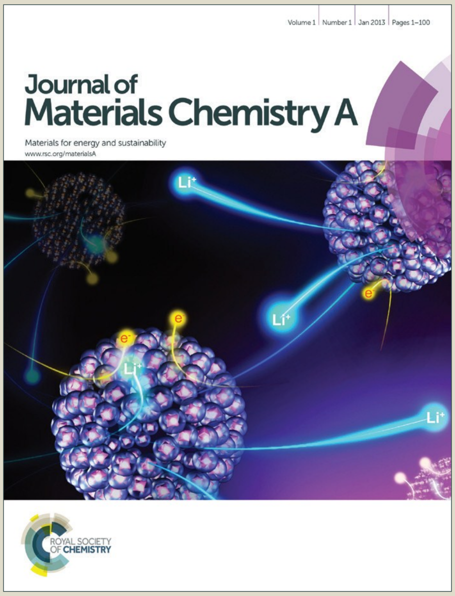

ROYAL SOCIETY OF CHEMISTRY

www.rsc.org/materialsA

Journal of Materials Chemistry A

ARTICLE

Silica Nanoparticles Catalyse the Formation of Silica Nanocapsules in a Surfactant-Free Emulsion System†

Received 00th January 20xx,
Accepted 00th January 20xx

DOI: 10.1039/x0xx00000x

www.rsc.org/

Yongliang Zhao,[ab] Zhi Chen,[a] Xiaomin Zhu*[ab] and Martin Möller[ab]

In this paper we report on a new green emulsification technique that utilizes a hydrophobic silica precursor polymer, hyperbranched polyethoxysiloxane (PEOS), for efficient stabilization of oil-in-water emulsions without any additional classical surfactants due to its hydrolysis-induced interfacial activity. Remarkably, in such an emulsion system methyl-functionalized silica nanoparticles can catalyze the conversion of PEOS to a mechanically strong silica shell at the oil/water interface. Thus, the oil phase is encapsulated in monodispersed silica nanocapsules with almost 100% efficiency. This process depends strongly on the pH value of the aqueous phase, which controls the interfacial activity of both PEOS and silica nanoparticles as well as PEOS hydrolysis and condensation. The catalytic effect of the silica particles is the result of a delicate interplay between their interfacial activity that allows immersing catalytically active silanolate groups in the PEOS-containing oil phase and the repulsion between charged surfaces of these particles and the resulting silica nanocapsules that splits them apart. We believe that this technique opens new avenues not only for the preparation of functional inorganic nanocapsules, but also for the design of a new type of heterogeneous catalysts.

Introduction

Micro- and nanocapsules are hollow micro- and nanoparticles consisting of a solid shell that surrounds a core-forming space available to entrap substances.[1] Micro- and nanoencapsulation finds numerous applications in various fields ranging from food and cosmetics to pharmacy and medicine, implementing protection and controlled release of active substances.[2-6] Organic polymers are the most widely used shell materials, and silica is a promising alternative owing to its chemical inertness, mechanical stability, biocompatibility, optical transparency and easy functionalization.[7,8]

A capsular structure often forms via a liquid core templating approach.[9-11] Emulsions including mini- and micro-emulsions are such templates employed to prepare capsular structures using interfacial reactions, and during these processes the dispersed aqueous or oil phase can be encapsulated with nearly 100% efficiency.[12-17] For instance, silica capsules were obtained from both water-in-oil (w/o) and oil-in-water (o/w) emulsions with tetraethoxysilane (TEOS) as the silica precursor.[18-20] Surfactants are usually to be added to warrant the emulsion stability. On the other hand, solid particles can also be employed instead of traditional surfactant molecules to stabilize emulsions[21,22] due to their interfacial activity.[23,24] These so-called Pickering emulsions can be used to create hollow structures named colloidosomes by fixing the stabilizing colloidal particles at the interface.[25-27] In these systems colloidal particles act not only as the emulsion stabilizing agent, but also as the building blocks of the resulting capsular structure, and the capsule size is mostly above 1 μm.

Recently, we developed a unique approach for the preparation of all-silica colloidosomes by gluing silica nanoparticles at the water-oil interface using a silica precursor polymer, hyperbranched polyethoxysiloxane (PEOS),[28] in both w/o and o/w Pickering emulsions.[29-31] The reason for PEOS being effective interfacial glue is the fact that it becomes adhered to the o/w interface upon hydrolysis. For both w/o and o/w systems silica nanoparticles are functionalized with long alkyl chains, and the modification degree in the w/o case is substantially higher. In the all-silica colloidosomes the silica particles form densely packed particle layers, indicating dominant attractive forces probably due to the hydrophobic interaction between the alkyl chains. It is generally accepted that the stability of Pickering emulsions is due to the coherent particle layer around the droplets that acts as a steric barrier against coalescence.[32,33] It has also been reported that repulsive colloidal particles, which give dilute planar monolayers on the droplet surface, can serve likewise as efficient emulsion stabilizers,[34-37] and the stabilization is explained by particle bridges.[34,37] In this work we initially attempt to combine methyl-functionalized silica nanoparticles

---

[a] DWI – Leibniz-Institute for Interactive Materials e.V. and Institute for Technical and Macromolecular Chemistry of RWTH Aachen University, Forckenbeckstrasse 50, Aachen, 52056, Germany. Email: zhu@dwi.rwth-aachen.de;

[b] Dutch Polymer Institute (DPI), P.O. Box 902, 5600 AX Eindhoven, The Netherlands.

† Electronic Supplementary Information (ESI) available: Hydrodynamic diameter distributions of silica nanoparticles and nanocapsules before and after centrifugation; FT-IR spectra of PEOS, silica nanoparticles, and dried silica nanocapsules; effect of shearing intensity during emulsification; Interfacial tension between a toluene solution of PEOS and an aqueous phase containing silica nanoparticles at different pH; FT-IR spectra of air-dried silica nanocapsules containing hexadecane and after the evaporation of hexadecane are supplied. See DOI: 10.1039/x0xx00000x

that are known to possess weak repulsion between each other[34] and PEOS in the o/w Pickering emulsions to prepare capsular structures with tailored surface coverage of particles and hence tailored permeability. To our great surprise, o/w emulsions can be stabilized solely by PEOS. Furthermore, under certain pH conditions the methyl-functionalized silica nanoparticles do not form colloidosomes with PEOS; instead, they catalyse the conversion of PEOS into mechanically stable silica nanocapsules.

Experimental

Materials

Tetraethoxysilane (TEOS, GPR RECTAPUR®, VWR), ammonia solution (28% EMSURE® ACS, Reag. Ph. Eur. zur Analyse, VWR), absolute ethanol (EMSURE® ACS, ISO, Reag. Ph. Eur. zur Analyse, VWR), toluene (AnalaR NORMAPUR® ACS, ISO, Reag. Ph. Eur. zur Analyse, VWR), acetic anhydride (ACS reagent, ≥98.0%, Sigma-Aldrich), hexadecane (ReagentPlus®, 99%, Sigma-Aldrich), ethoxytrimethylsilane (98%, ABCR) and titanium trimethylsiloxide (ABCR) were used as received. Deionized water was used for all experiments. PEOS was synthesized according to the method published elsewhere.[28] The resulting PEOS had the following characteristics: degree of branching 0.54, SiO_2 content 49.2 %, Mn 1740 and Mw/Mn 1.9 (measured by gel permeation chromatography in chloroform with evaporative light scattering detector calibrated using polystyrene standards).

Preparation of methyl-functionalized silica nanoparticles

A 500 mL flask was charged with TEOS (11.4 mL), ammonia aqueous solution (17.0 mL), and absolute ethanol (342 mL). The mixture was stirred on a magnetic stirrer at room temperature for 24 h. Afterwards, ethoxytrimethylsilane (30 µL) was added and the reaction mixture was stirred for additional 48 h. The particles were separated by centrifugation at 11000 rpm for 30 min on an Eppendorf centrifuge 5810 and rinsed three times with water. Finally, the particles were redispersed in water.

Preparation of silica capsules

Silica aqueous dispersion (10.0 g) was mixed with an oil phase containing PEOS (0.8 g), and then the mixture was emulsified using ultrasonic irradiation for 15 min (Branson Sonifier 450 cell disrupter, 3 mm microtip, 0.9 time circle, 247 W output). The resulting oil-in-water emulsion was gently stirred at room temperature for 3 days. The capsules were isolated by centrifugation, rinsed 3 times with water, and then redispersed in water for further measurements. The recipes for the capsule preparation are listed in Table S1†.

Characterization methods

Both hydrodynamic diameter and zeta potential were measured on a Malvern Zetasizer Nano Series. The hydrodynamic diameter was measured in a PS cell at a other[31] and PEOS in the o/w Pickering emulsions to prepare scattering angle of 147° at 25 °C. The zeta potential was measured in a universal dip cell in a PS cuvette for potential measurements at 25 °C. Before the measurements, the dispersions were diluted to a particle concentration of 1.5 wt ‰. Interfacial tension between the aqueous phase and the oil phase as a function of time was measured at room temperature on a DSA100 pendant drop tensiometer (Krüss, Germany). A drop of an aqueous dispersion of silica nanoparticles, initially contained in a syringe (1 mL) equipped with a needle (diameter ~ 1.8 mm), was pumped into an oil phase placed in an optical glass cuvette (10*10*45 mm). The interfacial tension was calculated by analysing the shape of the water droplet. Field-emission scanning electron microscopy (FE-SEM) experiments were performed on a Hitachi S4800 high-resolution field-emission scanning electron microscope with an accelerating voltage of 1.5 kV. Before measurements, the capsule dispersion was diluted to a desired concentration, and was then spin-coated on a silicon wafer substrate. The sample was air-dried under ambient conditions. In the case of cryogenic FE-SEM measurements, the electron microscope was equipped with a liquid-nitrogen-cooled sample preparation and transfer unit. A drop of a freshly prepared emulsion was placed on a sample holder and quickly frozen by liquid nitrogen. Afterwards it was transferred into a cooled sample chamber of -160 °C, and then into the microscope chamber. Transmission electron microscopy (TEM) measurements were carried out on a Zeiss Libra 120 TEM. The accelerating voltage was set at 120 kV. The samples were prepared by placing a drop of a diluted capsule dispersion on a Formvar-carbon-coated copper grid with 200 meshes. Fourier-Transform Infrared (FT-IR) spectra were recorded on a Nicolet 60 SXR FT-IR spectrometer using the KBr pellet technique. Thermal gravimetric analysis (TGA) measurements were conducted on a PerkinElmer STA 6000 unit operating under nitrogen atmosphere with a flow rate of 100 mL min^{-1}. The nanocapsules were isolated from the aqueous dispersions by centrifugation and air-dried overnight. 5-10 mg of the dried sample were placed in a standard PerkinElmer alumina 85 µL crucible for the measurements. Nitrogen adsorption-desorption measurements were carried out at 77 K on a QUADRASORB *SI* automated surface area & pore size analyser (Quantachrome Instruments, USA). The Brunauer-Emmett-Teller (BET) specific surface area was calculated using the adsorption data at a relative pressure range of P/P_0 = 0.05-0.3 and the pore size was calculated with the NL-DFT method using the desorption branch.

Results and discussion

Methyl-functionalized silica nanoparticles with an average diameter of 50 nm were obtained via the typical Stöber method[37] and subsequent addition of ethoxytrimethylsilane. The modification degree was adjusted so that the resulting particles could still be well-dispersible in water. The preparation of capsules was carried out according to a procedure described previously by us.[30] Briefly, a toluene solution of PEOS was emulsified in an aqueous dispersion of methyl-functionalized silica nanoparticles at pH 9 by ultrasonic treatment. Afterwards, the resulting emulsion was stirred at ambient temperature for 3 days. With 1.2 wt.-% silica particles in water (Run 1 in Table S1†), field-emission scanning electron microscopy (FE-SEM) and transmission electron microscopy (TEM) show the co-existence of nearly spherical silica nanocapsules and pristine silica nanoparticles in the reaction mixture without forming colloidosomes (Fig. 1). The silica nanocapsules can be isolated via centrifugation at 8000 rpm; meanwhile the silica nanoparticles remain in the supernatant (Fig. 1b and Fig. S1†). These capsules have a mean diameter of 310 nm and a very narrow size distribution. Their size is significantly smaller than that of the colloidosomes formed under the similar reaction conditions with hexadecyl-functionalized silica nanoparticles, which mostly exceeds 1 µm.[30] The hollow capsular structure is unambiguously confirmed by TEM and FE-SEM data. The FE-SEM image of a broken capsule (very rare) (inset in Fig. 1c) reveals not only the hollow structure, but also the morphology of the inner surface, which is decorated with 20 nm tiny dots. Such characteristic structural feature, which results from the phase separation of unhydrolysed TEOS because of limited contact with water, was reported previously.[38,39] In our system, the contact of PEOS molecules with water at the water-oil interface is limited, hence leading to the incomplete hydrolysis of PEOS. Indeed, the FT-IR spectrum of the dried silica nanocapsules (Fig. S2†) shows clearly the presence of a small amount of remaining ethoxysilane groups (absorption bands at 2800 – 3000 cm^{-1}). This is in contrast to the all-silica colloidosomes, where the hydrolysis according to the FT-IR spectra is fully completed.[29,30] Probably in this case, the hydrolysis and condensation of PEOS at the interface result in a dense outer silica shell that hinders the further diffusion of water molecules towards the unreacted ethoxysilane groups on the inner surface of the silica shell.

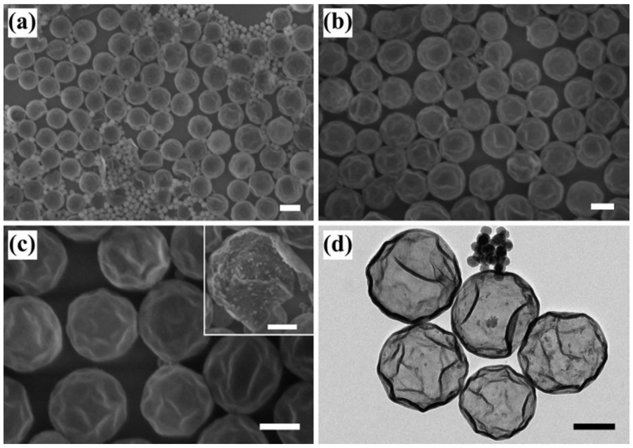

Fig. 1 (a) FE-SEM image of silica nanocapsules and co-existing silica nanoparticles obtained after drying the reaction mixture (Run 1 in Table S1†). (b) FE-SEM image of silica nanocapsules isolated using centrifugation. (c) High-magnification FE-SEM image of silica nanocapsules. The inset reveals the morphology of the inner surface of a broken capsule. (d) TEM image of silica nanocapsules. The scale bars represent 200 nm.

The average thickness of the silica shell d_s measured by TEM is 17 nm. d_s can also be estimated theoretically for this recipe, where the mass of PEOS and toluene is equal, using equation (1) assuming that the encapsulated substance is pure toluene, and it occupies the whole cavity of the capsule:

$$\left[\frac{4}{3}\pi R_c^3 - \frac{4}{3}\pi(R_c - d_s)^3\right]\cdot\rho_s = S\cdot m_{PEOS} = S\cdot m_t = S\cdot \frac{4}{3}\pi(R_c - d_s)^3\cdot\rho_t \qquad (1)$$

where R_c is the mean radius of the capsules and is measured to be 155 nm, ρ_s is the density of hydrated silica that equals 1.65 g cm^{-3},[40] ρ_t is the density of toluene and equals 0.867 g cm^{-3} and S is the silica content of PEOS, which is 49.2%. So d_s is calculated to be 11 nm, in quite a good agreement with the experimental data. Although the shell of the silica nanocapsules is wrinkled, very few broken capsules are observed by electron microscopy, indicating their outstanding integrity.

The silica capsules were prepared at various concentrations of silica nanoparticles by maintaining the other reaction conditions. As shown in Fig. 2, stable emulsions and capsular structures can be obtained in all cases. However, without silica particles, the capsules are collapsed and stuck to each other after drying, indicating the high softness of the shell most probably because of a lower conversion degree of PEOS. Prolongation of the reaction time does not result in noticeable hardening of the capsule shell. Interestingly, the mechanical strength of the silica shell improves significantly with the increase of the concentration of silica nanoparticles. At 1.2 wt.-% silica particles, the dried capsules are almost spherical with slight wrinkling of the shell. The further increase of the silica particle concentration leads solely to broadening of the size distribution without changing the capsule shape (Fig. 2f). Assuming that silica nanoparticles form a monolayer on the oil droplets, the average coverage of the droplets can be estimated using equation (2):[41]

$$R_o = Coverage\ \cdot\pi\cdot\left(\frac{W_o}{W_p}\right)\cdot\left(\frac{\rho_p}{\rho_o}\right)\cdot R_p \qquad (2)$$

where *Coverage* is the surface area of an oil droplet covered by silica particles; ρ_p and ρ_t are densities of silica particles and oil phase (PEOS in toluene), which equal 2.2 and 0.98 g cm^{-3}, respectively; R_p, R_o and W_p, W_o are radius and weight of silica particles and oil droplets, correspondingly. R_p is 25 nm. For the emulsion formed in water containing 1.2 wt.-% silica particles (Run 1 in Table S1†), R_o estimated from the capsule size is 174 nm, *Coverage* is then calculated to be only 14.8%. Such a small amount of silica nanoparticles is certainly not enough to form a coherent particle layer for a steric stabilization of such small emulsion droplets.

As demonstrated in our previous studies, upon hydrolysis of hydrophobic ethoxysilane to hydrophilic silanol groups the solubility of PEOS in hydrocarbons is reduced and its affinity towards water increases, so it becomes adhered to the oil-water interface.[29-31] Indeed, as depicted in Fig. 3, the interfacial tension (IFT) between the PEOS toluene solution and water decreases steadily with time and reaches a value as low as 9 mN/m, implying the continuous migration and hydrolysis of PEOS at the water-oil interface. So the partially hydrolysed PEOS behaves as an interfacial-active surfactant, as similar to hydrolysed long-alkyl-substituted alkoxysilanes[42,43] and poly(ethylene glycol)-functionalized PEOS.[44] By adding methylated silica nanoparticles into water, time needed for the IFT value to reach the plateau decreases significantly and shortens with the increase of the silica particle concentration. With 1.8 wt.-% silica particles in water, the IFT value starts even to grow after 200 s. It seems that the IFT of these systems is mainly defined by the hydrolysed PEOS, the silica nanoparticles; on the other hand, influence the kinetics of the formation of the surfactant monolayer at the interface by accelerating the hydrolysis of PEOS molecules. At a very high silica particle concentration, the monolayer of the hydrolysed PEOS molecules forms quickly, and meanwhile the condensation also takes place leading to the formation of a solid layer. Therefore, the apparent interfacial tension increases.

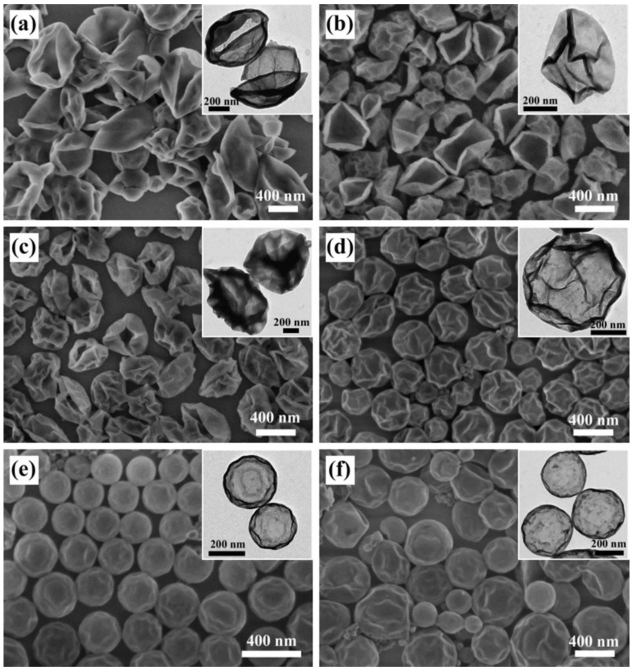

Fig. 2 FE-SEM images of capsules prepared with various concentrations of silica nanoparticles in water: (a-f) 0, 0.15, 0.3, 0.6, 1.2 and 1.8 wt.-%. The insets show the corresponding TEM micrographs.

The evolution of the reaction mixture with time was followed by dynamic light scattering (DLS) measurements. After ultrasonic emulsification, the DLS data of the reaction mixture (Fig. 4a) show two broad overlapping peaks that most probably correspond to the silica nanoparticles and the emulsion droplets. The cryo-FE-SEM image of the freshly prepared emulsion (top left inset in Fig. 4a) shows that the droplets are bigger than the final silica capsules and the silica nanoparticles are adsorbed on their surface. After stirring for 12h, the peak intensity of the silica nanoparticles decreases and that of the droplets increases. It can be related to the increased attachment of the silica particles on the droplet surface. The FE-SEM micrograph also shows the not completely solidified capsule shells surrounded by the silica nanoparticles (Fig. 4b). As the PEOS condensation proceeds further, the intensity of the peak corresponding to the silica particles increases, indicating that they are split from the capsule surface.

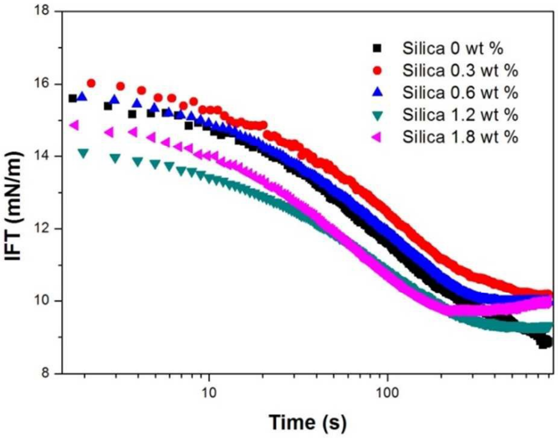

Fig. 3 IFT of a toluene solution of PEOS (weight ratio of PEOS to toluene is 1:1) in water at pH 9 containing different concentration of silica nanoparticles *versus* time.

Since the size of the original emulsion droplets is close to 500 nm, the emulsions formed with PEOS can be considered as miniemulsions. Indeed, they are formed only under high-energy ultrasonication (Fig. S3†). This high-powered homogenization step creates submicrometer droplets, ensuring not only a large contact area between PEOS and water, but also redistributing rather than permanently trapping of the silica nanoparticles at the water-oil interface. Thus, PEOS can be quickly hydrolysed to become interfacial-active. The high stability of the resulting miniemulsions can probably be attributed to electrostatic repulsion of the dissociated silanol groups at pH 9 and a barrier layer formed by partially hydrolysed and partially condensed PEOS on the oil droplet surface, preventing Ostwald ripening. As shown by the DLS data (Fig. 4a), during the first 12 h of the reaction, more particles become attached to the droplet surface as a result of the condensation of the surface silanol groups with PEOS. These particles can provide additional stabilization of the emulsion droplets. However, upon solidification of the capsules, they are detached from the capsule surface. By comparing with our previous study where hexadecyl-functionalized silica nanoparticles were used to stabilize the o/w Pickering emulsions and they were glued together with PEOS to form silica colloidosomes of several micrometers,[30] the surface substitution of the silica nanoparticles seems to play a crucial role in defining the morphology of the capsule structure. We believe that owing to the strong hydrophobic interaction, the long alkyl chains tend to be located close to each other during the synthesis, forming a Janus-like structure. The methyl groups, however, are distributed homogeneously on the surface of the silica nanoparticles due to the weak interaction between them. It is well known that Janus particles that combine the amphiphilicity inherent to surfactants with the particle characteristics have a much higher interfacial activity than uniformly wetted particles.[45] Therefore, when the long-alkyl-functionalized Janus-like silica particles are used, the emulsions are stabilized predominantly by these particles that form a dense particle layer at the interface, and PEOS acts only as glue. The much less interfacial-active methylated silica nanoparticles, in contrast, cannot be firmly attached to the interface, so the hydrolysed PEOS molecules dominate over the particles in the emulsion stabilization.

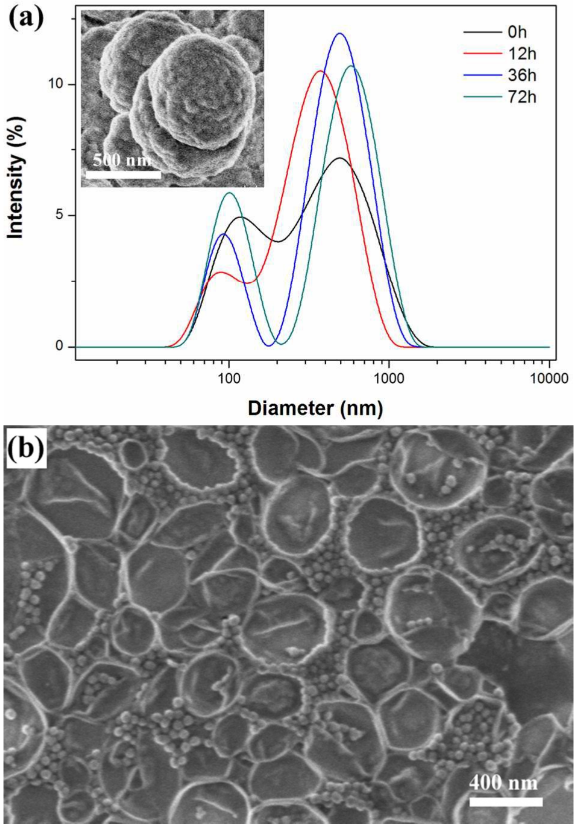

Fig. 4 (a) Evolution of size distribution of a reaction mixture (Run 1 in Table S1†) with time measured by dynamic light scattering. The top left inset shows a cryo-FE-SEM image of freshly prepared emulsion droplets that are decorated with silica nanoparticles; (b) FE-SEM image recorded for this mixture after stirring for 12h.

Both long-alkylated and methylated silica nanoparticles can facilitate the conversion of PEOS into silica. In the case of silica colloidosomes, the full conversion of PEOS was clearly demonstrated by FT-IR spectroscopy data, but the particles became the building blocks of the capsules.[29-31] For the system with methylated silica nanoparticles, as shown by the DLS and electron microscopy data, the particles indeed catalyse the PEOS conversion by first attaching and later leaving the capsules surface. The catalytic activity of silica particles in heterogeneous systems was shortly mentioned in the literature; however, no explanation was provided.[46] The mechanism we propose is schematically depicted in Fig. 5. The catalytic activity of the silica nanoparticles most probably originates from their interfacial activity. At pH 9 the zeta-potential of the methylated silica nanoparticles in water was measured to be -40.2 mV, indicating a high degree of ionic dissociation of surface silanol groups. In the aqueous solution, the silanolate groups are hydrated, so their nucleophilicity is significantly reduced. However, at the water-oil interface the particles are partially embedded in the oil phase. The surface silanolate groups that are immersed in the oil phase are naked, so they can exhibit a strong nucleophilicity to catalyse the conversion of PEOS into silica. There might be two reasons why the silica nanoparticles are not stuck on the surface of the formed silica nanocapsules. First of all, both silica nanoparticles and nanocapsules are negatively charged at pH 9, so the repulsive force can tear them apart. Their comparable size might be the second reason, thus the adhesion of the nanoparticles onto the nanocapsules could lead to the appearance of energetically unfavourable negative surface curvature.[7]

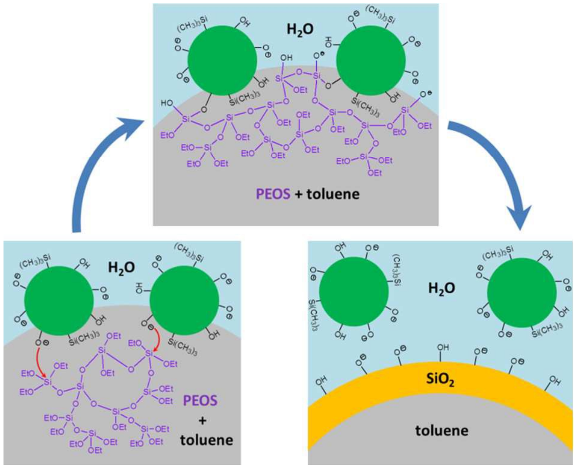

Fig. 5 Illustration of catalytic effect of methylated silica nanoparticles on the conversion of hyperbranched polyethoxysiloxane (PEOS) at the water-toluene interface.

The surface charge of silica particles is controlled by the pH value of aqueous media with the isoelectric point (IEP) at pH 2.0.[7] Furthermore, the pH also influences the kinetics of the hydrolysis and condensation of PEOS.[29,30,47] At a fixed concentration of silica nanoparticles (1.2 wt.-%), the effect of the pH of the aqueous phase that was adjusted by hydrochloric acid or ammonia solution on the capsule formation was investigated (Run 7-15 in Table S1†), and the obtained results are summarized in Fig. 6 and Table 1. At all studied pH values from 1.7 to 10.1, o/w emulsions are formed after ultrasonication, however, the pH value has a profound influence on the emulsion stability as well as the final capsule structure. At pH 1.7, the emulsion remains stable during 3 days stirring. According to the FE-SEM data, silica capsules without attached particles are obtained (Fig. 6a), although their size is 1.23 ± 0.11 μm, substantially bigger than that prepared at pH 9 (Fig. 1). With a slight increase of the pH value the silica nanoparticles start to be adsorbed onto the capsule surface and microsized colloidosomes are formed at pH 2-3 (Fig. 6b and 6c), although creaming takes place. At pH 4-5, the emulsions are broken after 3 days stirring, and fragments covered with silica nanoparticles are observed by FE-SEM (Fig. 6d and 6e). Further increase of pH leads again to stable emulsions. At neutral pH, however, FE-SEM shows broken capsules with the size less than 600 nm, indicating the low

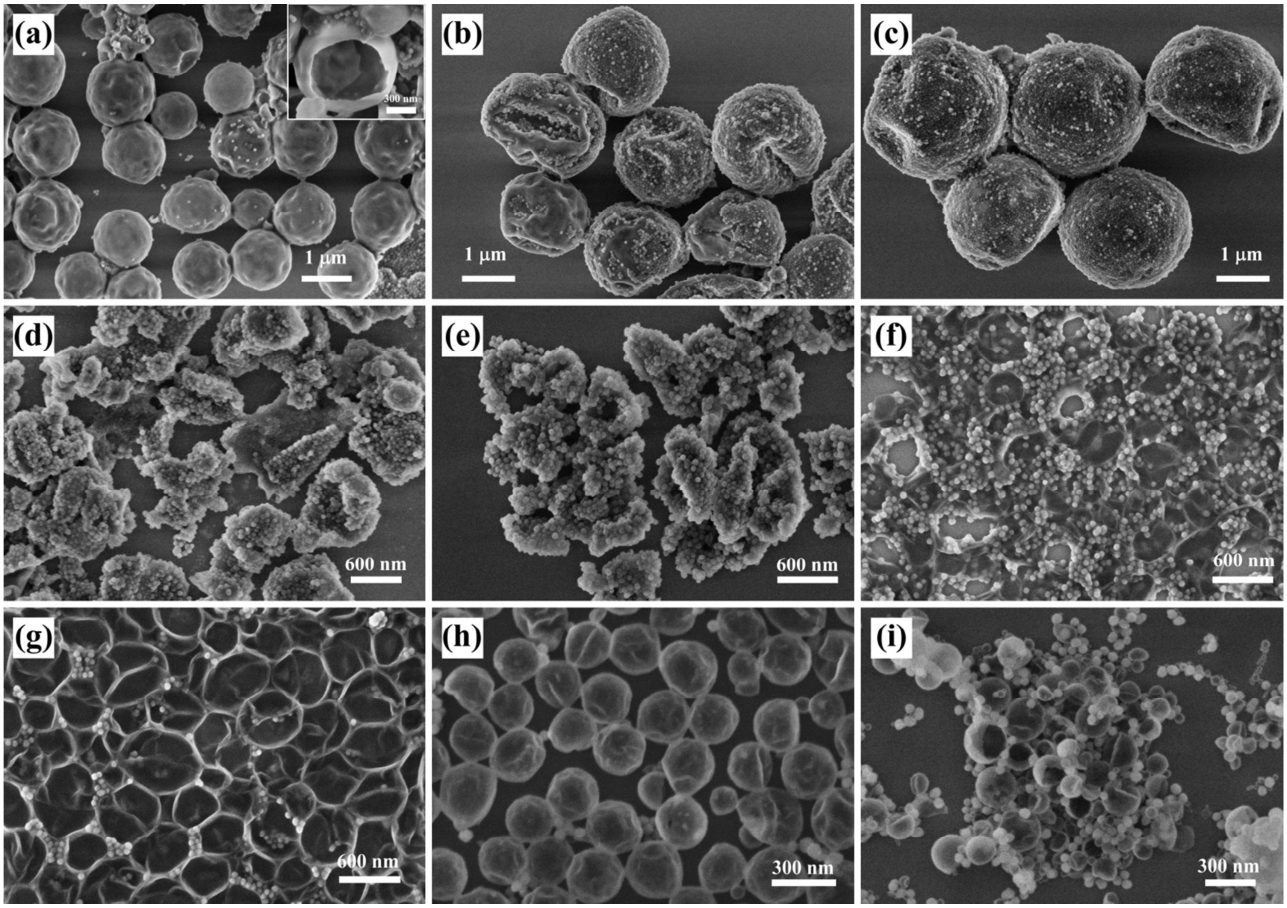

Fig. 6 FE-SEM images of final structures with different pH values of the aqueous phase: (a) 1.7, (b) 2.3, (c) 3.0, (d) 4.3, (e) 5.2, (f) 7.0, (g) 8.3, (h) 9.6, and (i) 10.1. A broken capsule is shown in the top right inset of (a) viewing the particle-free inner surface of the capsule shell.

mechanical strength of the shell (Fig. 6f and 6g). Mechanically strong particle-free silica nanocapsules are formed in a narrow pH range of 9-10, and the capsule size decreases with the increase of the pH. At pH 10.1, the emulsion is broken within 1-2 h and the co-existence of open silica nanocapsules and nanoparticles is observed after 3 days sol-gel reaction (Fig. 6i).

The charge can have a significant effect on the interfacial activity of both silica particles and hydrolysed PEOS. Upon the reduction of the charge, i.e. protonation of silanolate groups, the amphiphilicity and consequently the interfacial activity of the partially hydrolysed PEOS decrease, at the same time, the silica particles become more hydrophobic and energetically more favourable to be situated at the o/w interface compared with bulk.[32] At a very low pH (e.g. 1.7), the agglomeration of silica nanoparticles in water is so significant that they participate neither in the emulsion stabilization nor in the capsule formation process. The emulsion in this case is stabilized only by PEOS. Indeed, the same capsules are formed at this pH in the absence of any preformed silica nanoparticles. The big capsule size is probably due to the nonionic character of the hydrolysed PEOS molecules at this pH. Apparently, these molecules stabilize the emulsion droplets not as efficiently as the ionic ones formed at a high pH. In the pH range of 2-6, our experiments show that the o/w emulsions can be formed in

Journal of Materials Chemistry A

ARTICLE

Table 1 Role of polyethoxysiloxane (PEOS) and methylated SiO_2 nanoparticles in emulsion stabilization and capsule formation under different aqueous pH conditions.

	Aqueous pH				
	1.7	2.3 3.0	4.3 5.2 7.0	8.3 9.6	10.1
Methylated SiO_2 nanoparticles	Decrease of interfacial activity with increasing pH ←				
	Agglomeration	Emulsion stabilizer		Interfacial catalyst	
PEOS	Increase of interfacial activity with increasing pH →				
	Emulsion stabilizer	Interfacial particle glue	Slow conversion	Emulsion stabilizer	Too fast conversion
Capsule morphology	Particle-free microcapsules	Colloidosomes	No capsule formation	Particle-free nanocapsules	Broken capsules

the presence of the methylated silica nanoparticles without PEOS due to their increased interfacial activity as compared with that at higher pH values. So we speculate that the emulsions here are dominantly stabilized by the particles rather than PEOS. At pH 2-3 the hydrolysis and condensation of PEOS are fast enough to glue the particles together at the interface. In the pH range 4-7 the PEOS conversion is so slow that the emulsions are broken before the formation of colloidosomes. When the pH is above 7, the hydrolysed PEOS molecules start to dominate the emulsion stabilization. However, only when the pH is high enough, where the dissolution and redistribution reactions occur to provide a source of monomers required for monomer-cluster growth and to insure the achievement of reaction-limited conditions, a compact silica structure is formed.[47] At a too high pH (above 10), the conversion of PEOS is so fast that it loses quickly its amphiphilicity as indicated by the IFT measurements (Fig. S4†). The pH dependence of the behavior of the o/w emulsion system containing PEOS and methylated silica nanoparticles also confirms our explanation regarding the splitting of the silica nanoparticles from the nanocapsules after the solidification at pH 9. At low pH, where the surface charge is not significant and the capsule size is above 1 µm, the silica nanoparticles can stick to the capsule surface.

In order to study the release of substances encapsulated in the silica nanocapsules prepared at pH 9 under the catalysis of methyl-functionalized silica nanoparticles, a high boiling hydrophobic liquid, hexadecane, was enclosed (Run 16 in Table S1†). In this case, silica capsules with a diameter of 563 ± 65 nm, which is almost twice the size of the capsules prepared with toluene, are obtained (Fig. 7a). The bigger capsule size can be attributed to the higher interfacial tension of the hexadecane/PEOS/water system in comparison to that with toluene. By comparing the FT-IR spectra of the silica nanocapsule samples before and after the evaporation of hexadecane (Fig. S5†), which differ solely in characteristic bands of hexadecane, it is clearly affirmed that hexadecane is indeed encapsulated in the silica nanocapsules. Thermal gravimetric analysis (TGA) was used to study the encapsulation efficiency and release properties of the silica nanocapsules (Fig. 7b). The total weight loss upon heating is very close to the amount of hexadecane used in the preparation recipe, meaning almost 100% encapsulation efficiency. The non-linear isothermal release profile can be accounted for by the thickening of the capsule shell during the liquid evaporation caused by wrinkling. The activation energy of the evaporation of hexadecane calculated for the initial linear region of the weight loss curve using Arrhenius equation is 72.2 kJ mol^{-1}, which is higher than that of free hexadecane (59.8 kJ mol^{-1}) as well as hexadecane encapsulated in micro-sized colloidosomes (66.7 kJ mol^{-1}).[30] Therefore, it can be concluded that the silica nanocapsules developed in this work have good barrier properties. For the further characterization of the porous structure of the capsule wall nitrogen adsorption-desorption measurements were performed. The silica nanocapsules show a type IV nitrogen adsorption isotherm with a type H3 hysteresis loop[48] (Fig. 8), which was reported for silica nanorattles[49] and silica nanocapsules[50-53] with a mesoporous shell. The Brunauer-Emmett-Teller (BET) specific surface area was determined to be 255.87 m^2 g^{-1} using the adsorption data at a relative pressure range of P/P_0 = 0.05-0.3 and the pore size was calculated to be 2-4 nm with the NL-DFT method using the desorption branch, indicating the mesoporous structure of the silica shell.

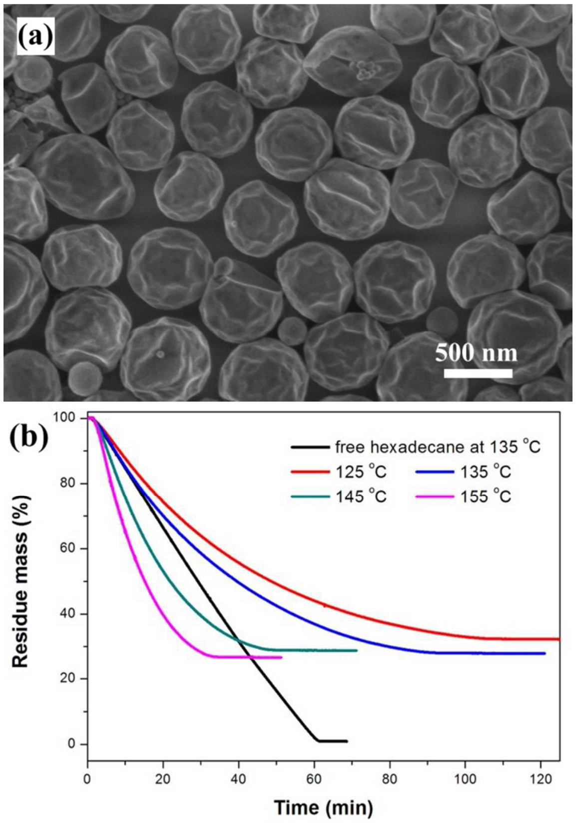

Fig. 7 (a) FE-SEM images of silica nanocapsules enclosing hexadecane (Run 16 in Table S1†) and (b) isothermal evaporation of free hexadecane and encapsulated hexadecane at different temperatures.

Conclusions

In summary, we have demonstrated that a hydrophobic precursor polymer PEOS becomes amphiphilic and interfacial active upon hydrolysis at the interface with water, thus being able to stabilize o/w (mini)emulsions without any additional surfactant. By employing the combination of PEOS and methylated silica nanoparticles in an oil/water binary system, different silica capsular structures ranging from particle-free microcapsules, colloidosomes and nanocapsules are obtained depending on the pH of the aqueous phase. Such diversity results from the pH-controlled interfacial activity of both PEOS and silica nanoparticles as well as PEOS conversion. Remarkably, at a relatively high pH (9-10) the hydrolysis-induced interfacial activity of PEOS leads to the formation of stable o/w miniemulsions, in which methylated silica nanoparticles catalyse both hydrolysis and condensation of PEOS at the water-oil interface to a mechanically strong silica thin film. Thus, the oil phase is encapsulated with almost 100% efficiency in silica nanocapsules with outstanding barrier properties. After solidification of PEOS, the silica nanoparticles are split from the capsule surface. This is in contrast to the silica colloidosomes formed at the same pH from PEOS with hexadecyl-functionalized silica nanoparticles, which are supposed to be Janus-like and much more interfacial-active. These particles dominate over PEOS in the o/w emulsion stabilization, and are linked by PEOS at the interface to form microsized silica colloidosomes. The catalytic effect of methylated silica nanoparticles can be explained by their interfacial activity that allows immersing catalytically active silanolate groups in the oil phase. After the formation of a solid silica shell, these particles are detached from the capsule surface due to the repulsion of negatively charged surfaces and the prevention of energetically unfavourable negative surface curvature. We believe that our finding opens a new gateway for the development of surfactant-free emulsion technology; furthermore it allows not only efficient enclosing active substances in inorganic micro- and nanocapsules, but also designing a new type of heterogeneous catalysts.

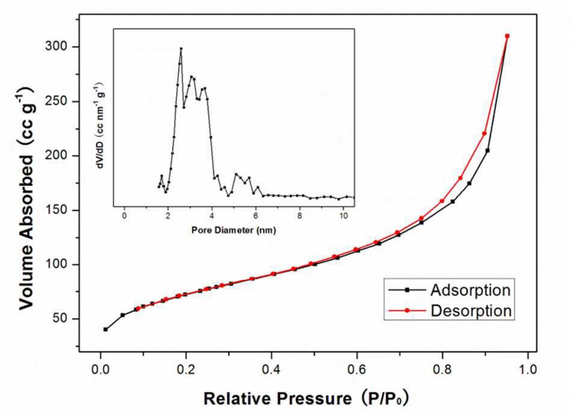

Fig. 8. Nitrogen adsorption-desorption isotherm and pore size distribution curve calculated with the NL-DFT method (insert) of dried silica nanocapsules.

Acknowledgements

This research forms part of the research programme of the Dutch Polymer Institute (DPI), project #747 NanoPA.

Notes and references

1 M. Vert, Y. Doi, K. H. Hellwich, M. Hess, P. Hodge, P. Kubisa, M. Rinaudo and F. Schue, *Pure Appl. Chem.*, 2012, **84**, 377-408.

2 R. Beck, S. Guterres and A. Pohlmann, *Nanocosmetics and Nanomedicines: New Approaches for Skin Care*, Springer, Berlin, Heidelberg, 2011.

3 S. Benita, *Microencapsulation: Methods and Industrial Applications*, Informa Healthcare, London, 2006.

4 P. N. Ezhilarasi, P. Karthik, N. Chhanwal and C. Anandharamakrishnan, *Food Bioprocess Tech.*, 2013, **6**, 628-647.

5 C. E. Mora-Huertas, H. Fessi and A. Elaissari, *Int. J. Pharm.*, 2010, **385**, 113-142.

6 X. W. Lou, L. A. Archer and Z. Yang, *Adv. Mater.*, 2008, **20**, 3987-4019.

7 R. K. Iler, *The Chemistry of Silica: Solubility, Polymerization, Colloid and Surface Properties and Biochemistry of Silica*, Wiley, New York, 1979.

8 M. Pagliaro, *Silica-based materials for advanced chemical applications*, RSC Pub., Cambridge, 2009.

9 H. N. Yow and A. F. Routh, *Soft Matter*, 2006, **2**, 940-949.

10 L. Han, P. Long, J. Bai and S. Che, *J. Am. Chem. Soc.*, 2011, **133**, 6106-6109.

11 Q. Yue, J. Li, Y. Zhang, A. A. Elzatahry, X. Wang, C. Wang, W. Li, X. Cheng, A. Alghamdi, A. M. Abdullah, Y. Deng and D. Zhao, *J. Am. Chem. Soc.*, 2015, **137**, 13282-13289.

12 C. I. Zoldesi and A. Imhof, *Adv. Mater.*, 2005, **17**, 924-928.

13 J. Fickert, P. Rupper, R. Graf, K. Landfester and D. Crespy, *J. Mater. Chem.*, 2012, **22**, 2286-2291.

14 J. Fickert, D. Schaeffel, K. Koynov, K. Landfester and D. Crespy, *Colloid Polym. Sci.*, 2014, **292**, 251-255.

15 Z. Cao, C. Xu, X. Ding, S. Zhu, H. Chen and D. Qi, *Colloid Polym. Sci.*, 2015, **293**, 1129-1139.

16 H. Pang, S. Zhou, L. Wu, M. Chen and G. Cu, *Colloids Surf., A*, 2010, **364**, 42-48.

17 B. Peng, M. Chen, S. Zhou, L. Wu and X. Ma, *J. Colloid Interface Sci.*, 2008, **321**, 67-73.

18 C. Barbe, J. Bartlett, L. G. Kong, K. Finnie, H. Q. Lin, M. Larkin, S. Calleja, A. Bush and G. Calleja, *Adv. Mater.*, 2004, **16**, 1959-1966.

19 R. Ciriminna, M. Sciortino, G. Alonzo, A. de Schrijver and M. Pagliaro, *Chem. Rev.*, 2011, **111**, 765-789.

20 F. Q. Tang, L. L. Li and D. Chen, *Adv. Mater.*, 2012, **24**, 1504-1534.

21 S. U. Pickering, *J. Chem. Soc., Trans*, 1907, **91**, 2001-2021.

22 W. Ramsden, *Proc. R. Soc. Lond.*, 1903, **72**, 156-164.

23 P. Finkle, H. D. Draper and J. H. Hildebrand, *J. Am. Chem. Soc.,* 1923, **45**, 2780-2788.

24 P. Pieranski, *Phys. Rev. Lett.*, 1980, **45**, 569-572.

25 A. D. Dinsmore, M. F. Hsu, M. G. Nikolaides, M. Marquez, A. R. Bausch and D. A. Weitz, *Science*, 2002, **298**, 1006-1009.

26 O. D. Velev, K. Furusawa and K. Nagayama, *Langmuir*, 1996, **12**, 2374-2384.

27 O. D. Velev, K. Furusawa and K. Nagayama, *Langmuir*, 1996, **12**, 2385-2391.

28 X. M. Zhu, M. Jaumann, K. Peter, M. Möller, C. Melian, A. Adams-Buda, D. E. Demco and B. Blumich, *Macromolecules*, 2006, **39**, 1701-1708.

29 H. L. Wang, X. M. Zhu, L. Tsarkova, A. Pich and M. Möller, *ACS Nano*, 2011, **5**, 3937-3942.

30 Y. L. Zhao, Y. Q. Li, D. E. Demco, X. M. Zhu and M. Möller, *Langmuir*, 2014, **30**, 4253-4261.

31 C. Zhang, C. Y. Hu, Y. L. Zhao, M. Möller, K. L. Yan and X. M. Zhu, *Langmuir*, 2013, **29**, 15457-15462.

32 B. P. Binks, *Curr. Opin. Colloid Interface Sci.*, 2002, **7**, 21-41.

33 D. E. Tambe and M. M. Sharma, *Adv. Colloid Interface Sci.*, 1994, **52**, 1-63.

34 T. S. Horozov and B. P. Binks, *Angew. Chem., Int. Ed.*, 2006, **45**, 773-776.

35 B. R. Midmore, *Colloids Surf., A*, 1998, **132**, 257-265.

36 E. Vignati, R. Piazza and T. P. Lockhart, *Langmuir*, 2003, **19**, 6650-6656.

37 W. Stöber, A. Fink and E. Bohn, *J. Colloid Interface Sci.*, 1968, **26**, 62-69.

38 H. Izutsu, F. Mizukami, P. K. Nair, Y. Kiyozumi and K. Maeda, *J. Mater. Chem.*, 1997, **7**, 767-771.

39 G. W. Scherer, *J. Non-Cryst. Solids*, 1989, **109**, 183-190.

40 M. J. Murtagh, E. K. Graham and C. G. Pantano, *J. Am. Ceram. Soc.*, 1986, **69**, 775-779.

41 T. Chen, P. J. Colver and S. A. F. Bon, *Adv. Mater.*, 2007, **19**, 2286-2289.

42 S. Sakamoto, A. Shimojima, K. Miyasaka, J. Ruan, O. Terasaki and K. Kuroda, *J. Am. Chem. Soc.*, 2009, **131**, 9634-9635.

43 A. Shimojima, Z. Liu, T. Ohsuna, O. Terasaki and K. Kuroda, *J. Am. Chem. Soc.*, 2005, **127**, 14108-14116.

44 H. L. Wang, G. Agrawal, L. Tsarkova, X. M. Zhu and M. Möller, *Adv. Mater.*, 2012, **25**, 1017-1021.

45 A. Walther and A. H. E. Müller, *Chem. Rev.*, 2013, **113**, 5194-5261.

46 R. D. Sonwalkar, C. C. Chen and L. K. Ju, *Bioresour. Technol.*, 2003, **87**, 69-73.

47 C. J. Brinker and G. W. Scherer, *Sol-Gel Science: The Physics and Chemistry and Materials Applications*, Academic Press, San Diego, 1990.

48 M. Kruk, M. Jaroniec, *Chem. Mater.*, 2001, **13**, 3169-3183.

49 D. Chen, L. L. Li, F. Q. Tang, S. O. Qi, *Adv. Mater.*, 2009, **21**, 3804-3807.

50 C. Zhang, K. L. Yan, C. Y. Hu, Y. L. Zhao, Z. Chen, X. M. Zhu, M. Möller, *J. Mater. Chem. B*, 2015, **3**, 1261-1267.

51 H. Blas, M. Save, P. Pasetto, C. Boissiere, C. Sanchez, B. Charleux, *Langmuir*, 2008, **24**, 13132-13137.

52 B. Tan, S. E. Rankin, *Langmuir*, 2005, **21**, 8180-8187.

53 Y. F. Zhu, Y. Fang, L. Borchardt, S. Kaskel, *Micropor. Mesopor. Mat.*, 2011, **141**, 199-206.

TOC

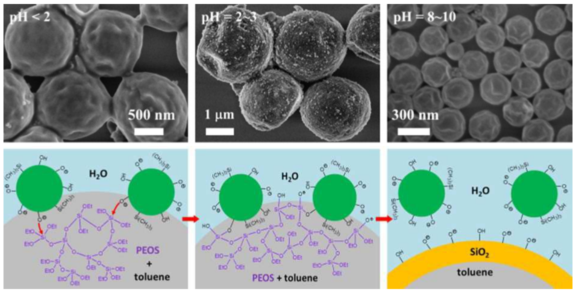

Interplay between methylated silica nanoparticles and polyethoxysiloxane at oil-water interface leads to a variety of silica capsule structures.